

ARTICLE OPEN



Trefoil factor 3 promotes pancreatic carcinoma progression via WNT pathway activation mediated by enhanced WNT ligand expression

Feifei Cheng ^{1,5}, Xuejuan Wang ^{1,5}, Yi-Shiou Chiou ^{1,2}, Chuyu He ¹, Hui Guo ¹, Yan Qin Tan ¹, Basappa Basappa ³, Tao Zhu ⁴, Vijay Pandey ^{1,2}✉ and Peter E. Lobie ^{1,2}✉

© The Author(s) 2022

Pancreatic ductal adenocarcinoma (PDAC) is a major cause of cancer-related mortality with a dismal prognosis that has changed little over the past few decades. Further understanding of the molecular pathology of PDAC progression is urgently required in order to improve the prognosis of patients with PDAC. Herein, it was observed that trefoil factor 3 (TFF3) expression was elevated in PDAC, and was positively correlated with a worse overall patient survival outcome. Forced expression of TFF3 promoted oncogenic functions of PDAC cells in vitro including cell proliferation, survival, foci formation, cancer stem cell-like behavior and invasion, ex vivo colony growth in 3D-Matrigel, and xenograft growth in vivo. Depletion or pharmacological inhibition of TFF3 inhibited these same processes. RNA-Seq analysis and subsequent mechanistic analyses demonstrated that TFF3 increased the expression of various WNT ligands to mediate WNT pathway activation required for TFF3-stimulated PDAC progression. Combined pharmacological inhibition of TFF3 and WNT signaling significantly attenuated PDAC xenograft growth and potentiated the therapeutic efficacy of gemcitabine in both ex vivo and in vivo models. Hence, a mechanistic basis for combined inhibition of pathways enhancing PDAC progression is provided and suggests that inhibition of TFF3 may assist to ameliorate outcomes in PDAC.

Cell Death and Disease (2022)13:265; <https://doi.org/10.1038/s41419-022-04700-4>

INTRODUCTION

The overall prognosis of patients with pancreatic ductal adenocarcinoma (PDAC) remains poor, with a 5-year survival rate of 8% [1]. Although a number of discrete genetic alterations associated with PDAC development and progression have been identified [2, 3], potent and non-mutated oncogenic drivers [4] that contribute to PDAC progression are still not well determined. Characterization of such oncogenes is necessary for expanding therapeutic strategies and prolonging the poor survival in patients with PDAC.

The human trefoil factor 3 (*TFF3*) gene encodes a small secreted protein of 59 amino acids with a trefoil structure [5]. TFF3 is a promiscuous ligand that activates multiple signaling pathways, including EGFR, CXCR4/7, HER2, MET, SRC, and IGF1R, and thus triggers downstream signaling of MAPK, PI3K/AKT, STAT3, and NF- κ B [4–6]. The cell surface receptors responsible for TFF3 function appear to be multiple and diverse with potential further TFF3 interacting proteins to be identified. Recently, CXCR4/7 [6], leucine-rich repeat receptor and nogo-interacting protein 2 (LINGO2) [7] and CD147 [8] have been implicated as potential receptors for TFF3.

Increasing evidence has indicated that TFF3 exerts crucial roles in the development and progression of various human cancers [4, 5, 9]. Indeed, TFF3 expression was reported to be elevated in colorectal [10–12], endometrial [13], gastric [14, 15], hepatocellular [16, 17], lung adeno- [18, 19], mammary [20–22], and prostate carcinomas [9, 23]. Increased TFF3 expression exerts pleiotropic effects that alter multiple biological processes involved in cancer development and progression. It has been demonstrated that TFF3 promotes cancer cell survival, proliferation, invasion, migration, angiogenesis, metastasis, and drug resistance [4, 18, 24–26]. In addition, increased expression of TFF3 is associated with poor prognosis of patients with various cancers, such as colorectal [27], gastric [14, 28, 29], hepatocellular [16], and mammary carcinomas [20, 30].

Whereas TFF3 has been suggested to exert pivotal functions in the development and progression of multiple cancers, the functions of TFF3 in PDAC have not been reported. Previous studies demonstrated significantly increased expression of TFF3 in human pancreatic carcinoma tissue [31, 32]. Similar results were also observed in the serum of patients with PDAC compared with

¹Tsinghua-Berkeley Shenzhen Institute and The Institute of Biopharmaceutical and Health Engineering Tsinghua Shenzhen International Graduate School, Tsinghua University, Shenzhen 518055, People's Republic of China. ²Shenzhen Bay Laboratory, Shenzhen 518055, People's Republic of China. ³Department of Studies in Organic Chemistry, University of Mysore, Mysore 570005, India. ⁴Department of Oncology of the First Affiliated Hospital of USTC, Division of Life Sciences and Medicine, University of Science and Technology of China, Anhui, Hefei 230027, People's Republic of China. ⁵These authors contributed equally: Feifei Cheng, Xuejuan Wang. ✉email: vijay.pandey@sz.tsinghua.edu.cn; pelobie@sz.tsinghua.edu.cn

Edited by Dr. Angelo Peschiaroli

Received: 24 October 2021 Revised: 10 February 2022 Accepted: 1 March 2022

Published online: 25 March 2022

benign controls [32]. Despite the above findings, the cellular functions, underlying molecular mechanisms, prognostic utility, and therapeutic potential of TFF3 in PDAC progression remain to be elucidated.

METHODS

Cells and reagents

Cell lines utilized in this study, their source, and culture are listed in Supplementary Table 1. For the generation of stable cell lines, Capan-1 and Panc-1 cells were transfected with empty *pIRESneo3-vector* or *pIRESneo3-TFF3* plasmid, and SW1990 cells were transfected with the control siRNA plasmid or siRNA plasmid targeting *TFF3* as previously described [20]. CTNNB1 in SW1990 cells was depleted using siRNA (#19761 and #19762) from Addgene (Cambridge, MA, USA). FuGENE® HD Transfection Reagent used for plasmid transfection was purchased from Promega (Madison, WI, USA). AMPC was synthesized in the Department of Studies in Organic Chemistry, University of Mysore.

Transcriptome analysis and tissue microarray

Transcriptome analysis of *TFF3* in human normal pancreatic tissues and PDAC was performed using the data from the publicly available database (OncoPrint, <https://www.oncoPrint.org/>). The tissue microarray (HPanA120Su02) was obtained from Outdo Bio-tech Co., Ltd. (Shanghai, China). Consent for the use of the tissue samples and clinical data were obtained by Outdo Bio-tech Co., Ltd. (Shanghai, China). The clinicopathological information of all cases is publicly available on the company website (<http://www.superchip.com.cn/>). Immunohistochemistry (IHC) staining and scoring were performed as previously described [33]. The corresponding antibodies used herein are listed in Supplementary Table 2. The staining results were assessed and confirmed by two independent researchers blinded to the clinical data.

Quantitative PCR (qPCR)

qPCR was performed as previously described [33]. β -ACTIN mRNA was used as input control. The sequences of the oligonucleotide primers used herein are listed in Supplementary Table 3.

RNA-seq

mRNA was isolated from cells using oligo(dT)-attached magnetic beads. RNA-seq was subsequently performed by BGI (Shenzhen, China) using the MGI2000 platform. The sequencing data were filtered with SOAPnuke (v1.5.2) followed by mapping to the reference genome using HISAT2 (v2.0.4). Differential expression analysis was performed using the DESeq2 (v1.4.5) with Q value ≤ 0.05 . Gene ontology (GO) and KEGG enrichment analysis were performed by Phyper based on a Hypergeometric test. Gene set enrichment analyses (GSEA) were performed using GSEA v3.0 software.

Serum and cell-based assays

TFF3 concentrations were measured by Quantikine® ELISA Human TFF3 Immunoassay kit (R&D Systems, USA) according to the manufacturer's protocol. Western blot and immunofluorescence analysis were processed as previously described [33]. The corresponding antibodies used are listed in Supplementary Table 2. Cell function assays were performed as previously described [20, 33, 34].

Xenografts

All animal experiments were approved by the Institutional Animal Care and Use Committee of the Laboratory Animal Centre of Peking University Shenzhen Graduate School (permit YW; the permit from Tsinghua Shenzhen International Graduate School is "Ethical Development no. 37 (year 2019)". Six-week-old male BALB/c athymic nude mice were grouped by simple randomization using a random number table method. The principle of sample size followed the "The ARRIVE Guidelines" [35]. Mice were subcutaneously injected with Capan-1-ctrl/TFF3 (1×10^7 cells) or SW1990-shctrl/shTFF3 (5×10^6 cells). For drug treatment, the mice were subcutaneously injected with SW1990 (5×10^6 cells). Six xenograft-bearing mice were each randomized into the vehicle, single-drug, double-drug, or triple-drug groups, and were treated with intraperitoneal injections of vehicle (1% DMSO/10%

PEG400 in normal saline), 20 mg/kg AMPC, 10 mg/kg ICG-001 (Selleck Chemicals, USA), or 5 mg/kg gemcitabine (Eli Lilly, USA). Xenograft volume was calculated as previously described [33]. Immunohistochemical analysis of xenograft histology sections was performed as previously described [30, 36].

Statistical analysis

Two-tailed unpaired Student's t test and ANOVA analysis were used to calculate the statistical significance of two or multiple treatment groups, respectively. As for overall survival analyses, Kaplan–Meier survival curves were used. The level of significance was set as $*P < 0.05$, $**P < 0.01$, and $***P < 0.001$. Normally distributed data were presented as mean \pm standard deviation.

RESULTS

TFF3 expression is increased in PDAC

TFF3 mRNA expression in human normal pancreatic tissues and PDAC from the publicly available data set was first examined. It was observed that *TFF3* mRNA expression in PDAC was significantly higher than in normal pancreatic tissues (Fig. 1A). The expression levels of TFF3 protein in PDAC tissues and cell lines were next examined. By IHC analysis, it was observed that TFF3 protein exhibited significantly increased expression in PDAC compared with normal pancreatic tissues (Fig. 1B, C). A high expression level of TFF3 was observed in 59.1% (39/66) of cancer tissue, whereas in normal tissue, high expression was observed in 24.1% (13/54) of samples (Fig. 1C). Notably, in normal pancreatic tissue, TFF3 protein was mainly expressed in pancreatic islets (Fig. 1B), consistent with that reported in previous studies [37, 38]. However, the expression of TFF3 protein in cancer tissue was predominately located in PDAC cells (Fig. 1B). Furthermore, the correlation between TFF3 protein expression and the clinicopathologic characteristics of patients with PDAC was assessed. It was observed that TFF3 expression was not related to gender, age, or histological grade, but was significantly associated with tumor size (Supplementary Table 4). Importantly, survival analysis revealed that high TFF3 expression was positively correlated with worse overall survival of PDAC patients compared with those patients with low expression of TFF3 (Fig. 1D).

It was also demonstrated that there was significantly higher *TFF3* mRNA expression in human PDAC cell lines compared with that in the normal human pancreatic duct epithelial (HPDE6-C7) cell line (Fig. 1E). Considering that TFF3 is a secreted protein, the extracellular TFF3 protein levels were further determined. The results indicated that the PDAC cell lines exhibited higher concentrations of extracellular TFF3 protein compared with the HPDE6-C7 cell line (Fig. 1F). These findings provide further confirmatory evidence that TFF3 expression is increased in human PDAC.

Forced expression of TFF3 promotes oncogenicity of PDAC cells

In order to determine the cellular function of TFF3 in PDAC progression, Capan-1 and Panc-1 cell lines with stable forced expression of TFF3 (designated as Capan-1-TFF3 and Panc-1-TFF3) were established. The enhanced expression of TFF3 was verified by qPCR and Western blot analysis (Fig. S1A, B, and S01). Subsequently, the effect of forced expression of TFF3 on PDAC cell proliferation was examined by total cell number and BrdU incorporation assays. Forced expression of TFF3 enhanced the proliferative capability of Capan-1 cells compared with the control cells (Figs. 2A and S1C). Similar results were observed in Panc-1 cells (Figs. 2A and S1C). It was also observed that forced expression of TFF3 in Capan-1 and Panc-1 cells markedly promoted cell-cycle progression and suppressed apoptosis (Figs. 2B, C, S1D, E). Moreover, forced expression of TFF3 increased foci formation of Capan-1 and Panc-1 cells (Fig. 2D). Three-dimensional (3D) Matrigel assays were used to examine the effect of forced

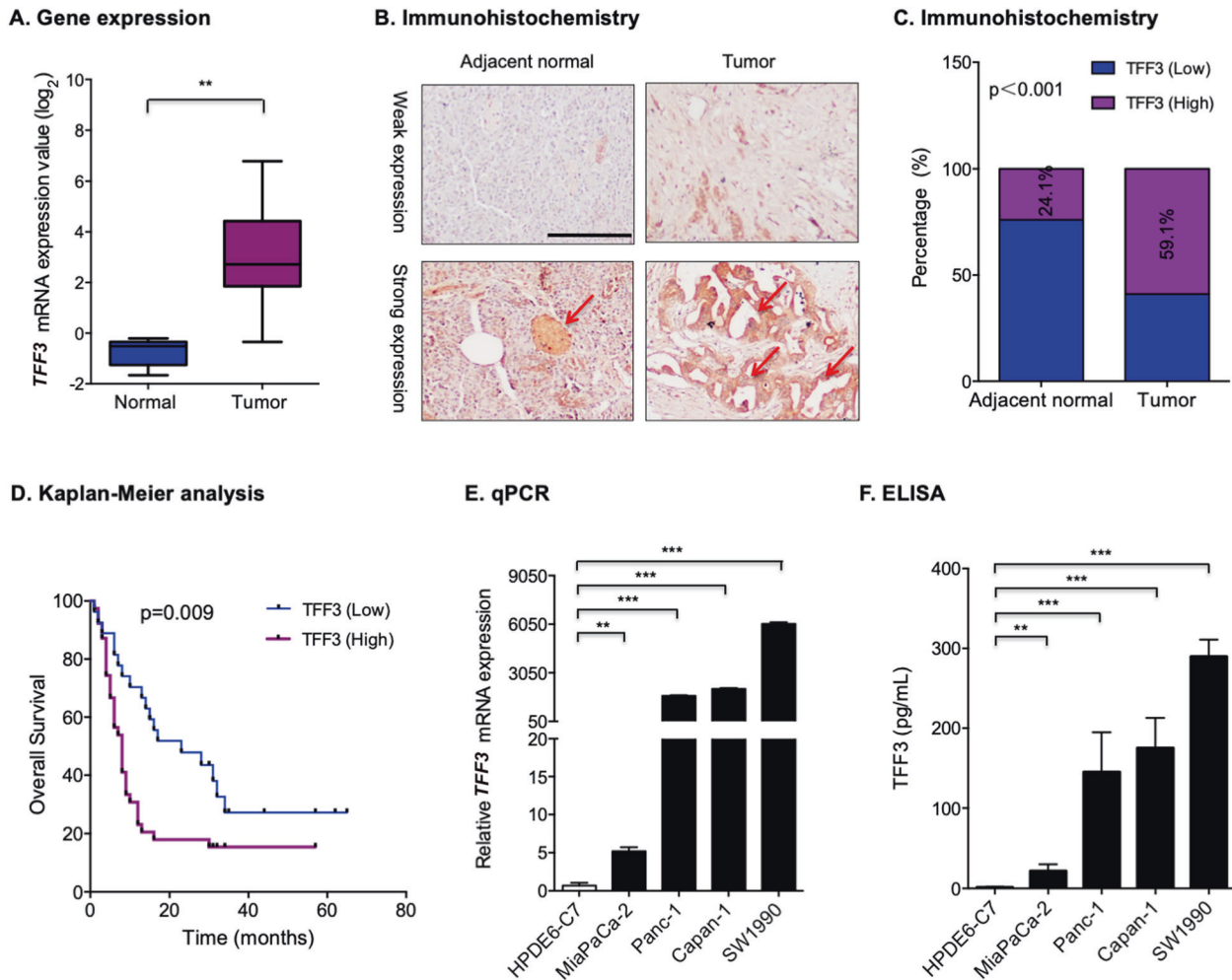


Fig. 1 TFF3 expression was increased in PDAC. **A** Transcriptomic analysis of *TFF3* via a publicly available database (Oncomine). Data represent means \pm SD. * $P < 0.05$, ** $P < 0.01$, and *** $P < 0.001$. **B** IHC analysis for TFF3 protein expression in PDAC and normal tissues. Representative IHC images of TFF3 expression in adjacent normal and tumor tissues are shown. Scale bar, 20 μ m. **C** The percentage of high versus low expression of TFF3 in the adjacent normal and tumor tissues. **D** Kaplan–Meier analysis of overall survival in PDAC stratified according to TFF3 low or high expression in PDAC tissues. **E** qPCR analysis for *TFF3* mRNA expression levels in human normal and PDAC cell lines. **F** ELISA analysis of extracellular TFF3 protein levels in human normal and PDAC cell lines.

expression of TFF3 on the 3D growth of PDAC cells. The colonies formed by Capan-1–TFF3 and Panc-1–TFF3 cells were significantly more numerous and larger compared with the respective control cells, suggesting that forced expression of TFF3 promoted 3D growth of PDAC cells (Fig. 2E). In addition, Capan-1–TFF3 cells also exhibited a significant increase in migration and invasion compared with the control cells (Fig. S1F, G).

Next, it was determined whether forced expression of TFF3 accelerated PDAC growth in vivo using a mouse xenograft model. Forced expression of TFF3 significantly increased the xenograft volume and weight at the termination of the experiment (Fig. 2F, G). The retention of increased expression of TFF3 in xenografts derived from Capan-1–TFF3 cells was demonstrated by IHC analysis (Fig. S1H). IHC analysis further revealed that forced expression of TFF3 in PDAC cells markedly increased the proportion of Ki67-positive cells (Fig. 2H). In addition, forced expression of TFF3 in PDAC cells also significantly reduced apoptosis (Fig. 2I). Hence, forced expression of TFF3 facilitates PDAC progression in vitro and in vivo.

Depletion of TFF3 suppresses oncogenicity of PDAC cells

TFF3 was depleted in SW1990 cells via a siRNA-based approach (designated as SW1990-shTFF3). The depletion efficiency of TFF3 was

determined by qPCR and western blot analysis (Fig. S2A, B, and S2O). It was observed that depletion of TFF3 significantly inhibited the proliferation of SW1990 cells (Figs. 3A and S2C). Depletion of TFF3 in SW1990 cells also significantly suppressed cell-cycle progression and promoted apoptosis (Figs. 3B, C, S2D, E). Furthermore, depletion of TFF3 impaired foci formation and 3D growth of SW1990 cells (Fig. 3D, E) as well as decreased migration and invasion (Fig. S2F, G).

As shown in Fig. 3F, G, depletion of TFF3 in SW1990 cells significantly reduced xenograft volume and weight at the termination of the experiment. The retention of TFF3 depletion in xenografts was confirmed using IHC analysis (Fig. S2H). IHC analysis further revealed that depletion of TFF3 in SW1990 cells resulted in reduced proliferation and increased apoptosis of cancer cells (Fig. 3H, I). Hence, depletion of TFF3 suppresses PDAC progression in vitro and in vivo.

AMPC suppresses the oncogenicity of PDAC cells

TFF3 has been reported to form disulfide-linked dimers with itself or other proteins via the seventh cysteine (Cys57) residue [10, 39]. The monomeric and dimeric forms of TFF3 exhibit differences in cellular functions [39]. Notably, the homodimeric form of TFF3 was reported to be essential for the pro-proliferative and anti-apoptotic functions of TFF3 [10]. A small-molecule inhibitor of

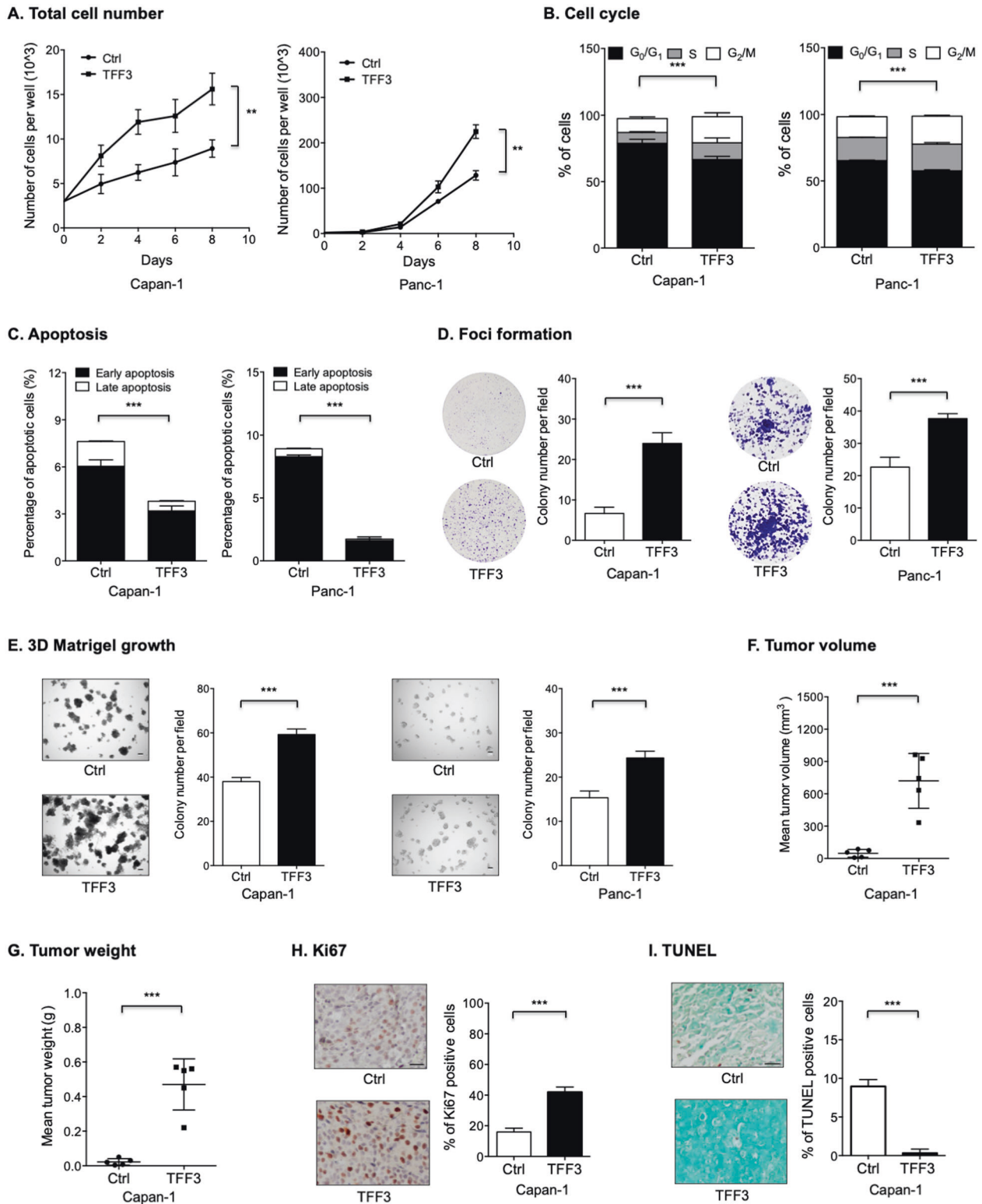


Fig. 2 Forced expression of TFF3 promoted oncogenicity of PDAC cells. **A** Total cell number analysis was performed to determine the effect of forced expression of TFF3 on cell proliferation in Capan-1 and Panc-1 cells. **B** Cell-cycle progression change of Capan-1 and Panc-1 cells after forced expression of TFF3 was determined using PI staining followed by FACS analysis. The percentages of cells in each cell-cycle phase were plotted. **C** Apoptosis of Capan-1 and Panc-1 cells after forced expression of TFF3 was determined using AnnexinV/PI staining followed by FACS analysis. The percentages of cells in an early or late apoptotic phase were plotted. **D** Foci formation assay was performed to determine the effect of forced expression of TFF3 on foci formation by Capan-1 and Panc-1 cells. **E** 3D-Matrigel analysis was performed to determine the effect of forced expression of TFF3 on 3D growth of Capan-1 and Panc-1 cells. Scale bar, 50 μ m. **F–G** The volume (**F**) and weight (**G**) of xenografts formed by Capan-1-TFF3 or the control cells at the termination of the experiment. **H** Representative micrographs and quantitative assay of IHC staining for Ki67 in the indicated xenografts. Scale bar, 20 μ m. **I** Representative micrographs and quantitative assay of TUNEL staining in the indicated xenografts. Scale bar, 20 μ m.

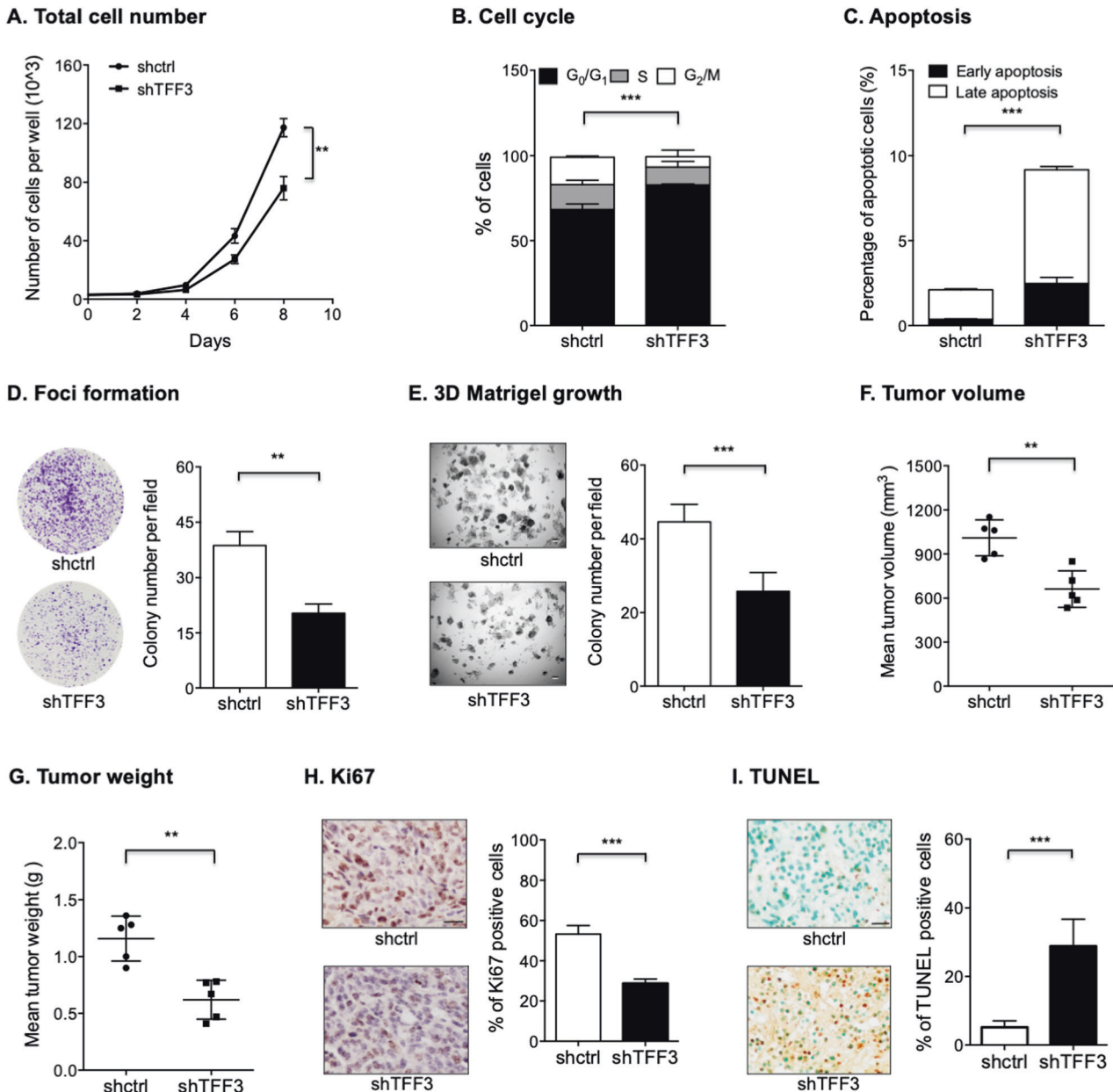


Fig. 3 Depletion of TFF3 suppressed oncogenicity of PDAC cells. **A** Total cell number analysis was performed to determine the effect of depletion of TFF3 on cell proliferation in SW1990 cells. **B** Cell-cycle progression of SW1990 cells after depletion of TFF3 was determined using PI staining followed by FACS analysis. The percentages of cells in each cell-cycle phase were plotted. **C** Apoptosis of SW1990 cells after depletion of TFF3 was determined using AnnexinV/PI staining followed by FACS analysis. The percentages of cells in an early or late apoptotic phase were plotted. **D** Foci formation assay was performed to determine the effect of depletion of TFF3 on foci formation of SW1990 cells. **E** 3D-Matrigel analysis was performed to determine the effect of depletion of TFF3 on 3D growth of SW1990 cells. Scale bar, 50 μ m. **F–G** The volume (**F**) and weight (**G**) of xenografts formed by SW1990-shTFF3 and the control cells at the termination of the experiment. **H** Representative micrographs and quantitative assay of IHC staining results for Ki67 in the indicated xenografts. Scale bar, 20 μ m. **I** Representative microscopic pictures and quantitative assay of TUNEL staining results in the indicated xenografts. Scale bar, 20 μ m.

TFF3 (designated as AMPC) that monomerizes homodimeric TFF3 was previously generated [10, 18].

The IC_{50} value of AMPC in multiple PDAC cell lines was determined using total cell number assays. It was observed that the IC_{50} value of AMPC in SW1990 cells with the highest endogenous TFF3 expression was significantly lower than those in other cell lines (Figs. 1E and S3A). AMPC treatment significantly impaired the proliferative capability of SW1990 cells in a dose-dependent manner (Fig. 4A). Similar results were observed in Capan-1 cells (Fig. 4A). It was also observed that AMPC treatment markedly increased apoptosis of SW1990 and Capan-1 cells (Figs.

4B and S3B). In addition, AMPC treatment significantly impaired foci formation and 3D growth of PDAC cells (Fig. 4C, D), similar to that previously observed after depletion of TFF3 (Fig. 3D, E). Notably, AMPC treatment attenuated the increased 3D growth capacity resulting from forced expression of TFF3 in Capan-1 cells (Fig. 4E). Hence, pharmacological inhibition of TFF3 suppresses the oncogenicity of PDAC cells.

TFF3 induces WNT ligand expression in PDAC

To further explore the potential signaling mechanisms responsible for the oncogenic functions of TFF3 in PDAC progression, RNA-

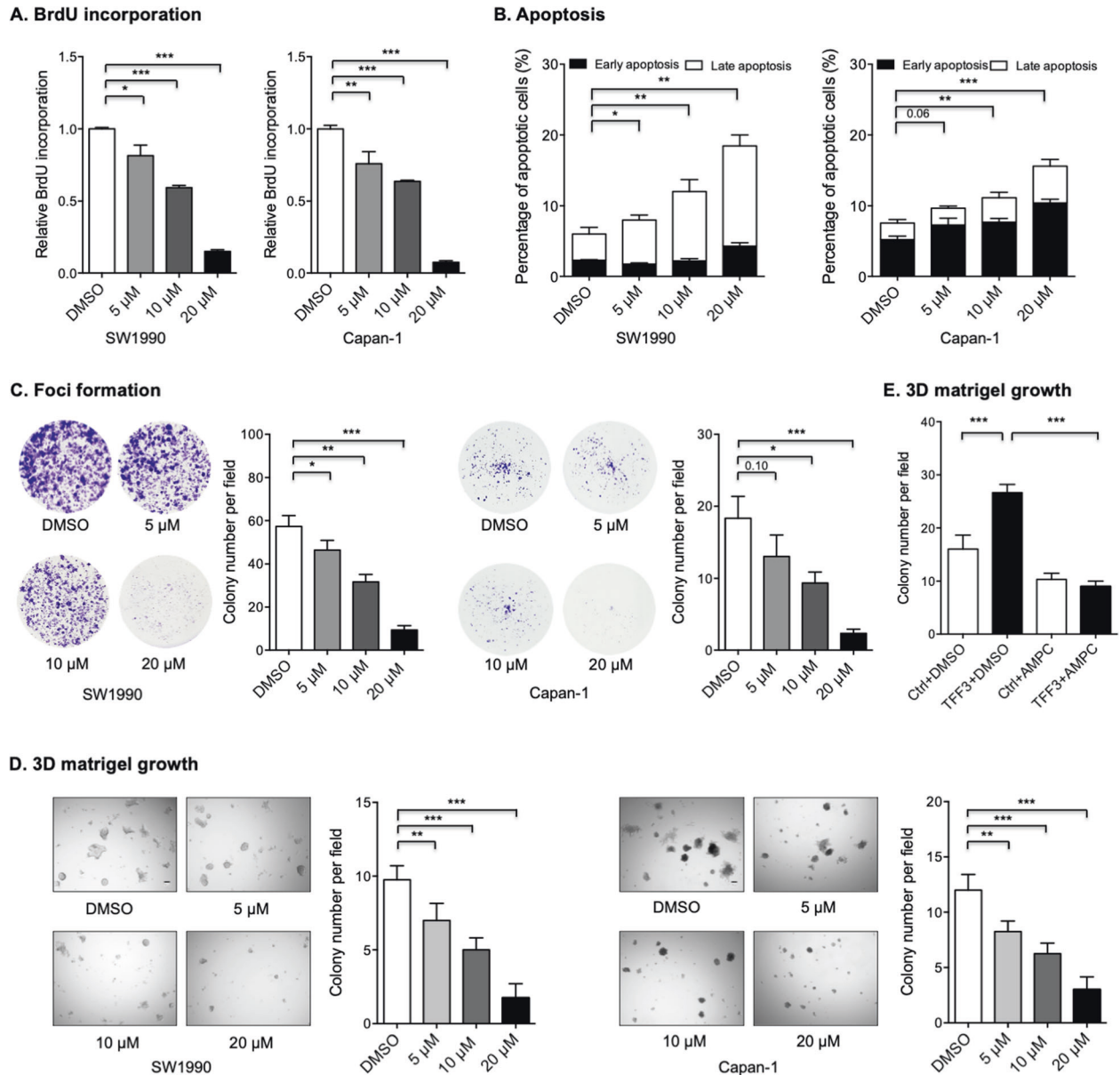


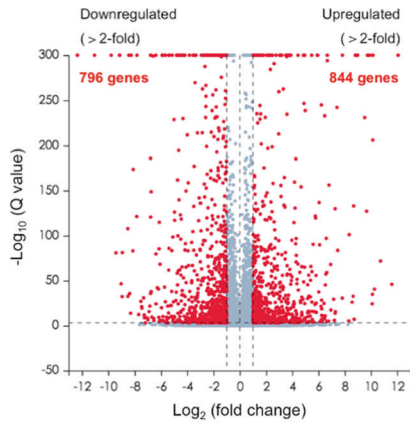
Fig. 4 AMPC suppressed oncogenicity of PDAC cells. **A** BrdU assay showed that AMPC treatment for 48 hours inhibited the proliferative capability of SW1990 and Capan-1 cells in a dose-dependent manner. **B** Apoptosis after AMPC treatment for 48 hours was determined using AnnexinV/PI staining followed by FACS analysis. The percentages of cells in the early or late apoptotic phase are plotted. **C** Foci formation assay showed that AMPC treatment for attenuated foci formation of SW1990 and Capan-1 cells in a dose-dependent manner. **D** 3D-matrigel growth analysis showed that AMPC treatment attenuated 3D growth of SW1990 and Capan-1 cells in a dose-dependent manner; **E** 3D-matrigel growth analysis showed that AMPC treatment abrogated the increased 3D growth produced by forced expression of TFF3 in Capan-1 cells.

sequencing (RNA-seq) was performed to characterize the transcriptome of Capan-1-TFF3 cells in comparison to the control cells. Gene expression analysis identified 1640 differentially expressed genes (fold change > 2), including 796 downregulated genes and 844 upregulated genes in Capan-1-TFF3 cells (Fig. 5A). GO analysis further indicated that many modulated genes were associated with the extracellular space (Fig. S4A). Consistently, gene set enrichment analysis further revealed that the genes with differential expression showed significant enrichment for “secreted factors” and “core matrisome” (Figs. 5B and S4B), both of which are closely associated with the extracellular space. Furthermore, KEGG-pathway analysis identified highly altered expression in several pathways; the most altered pathways included Hedgehog, TGF- β , and WNT signaling pathways (Fig.

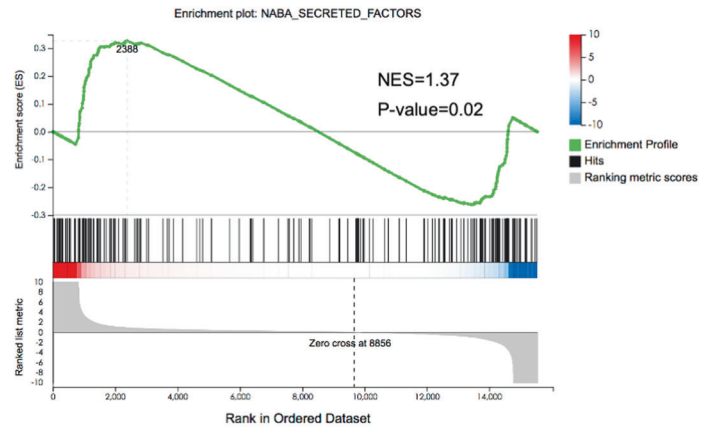
5C). As the WNT pathway has been shown to possess critical functions in PDAC progression [40], WNT-associated alterations in Capan-1-TFF3 cells were investigated. It was observed that multiple WNT ligands, such as *WNT1/6/7A/8A/8B/10A/10B&16*, exhibited significantly increased expression in Capan-1-TFF3 cells compared with those in the control cells (Fig. 5D), suggesting that TFF3 enhanced WNT ligand expression.

qPCR was, therefore, performed to verify WNT ligand mRNA expression changes after forced expression of *TFF3* in Capan-1 cells. As shown in Fig. 5E, forced expression of *TFF3* in Capan-1 cells significantly increased the expression of multiple WNT ligands, including *WNT1/3/4B/6/7A/7B/8A/9B/10A/10B&11*. In addition, western blot analysis showed that forced expression of *TFF3* in Capan-1 cells also enhanced the expression of WNT1/3&8A

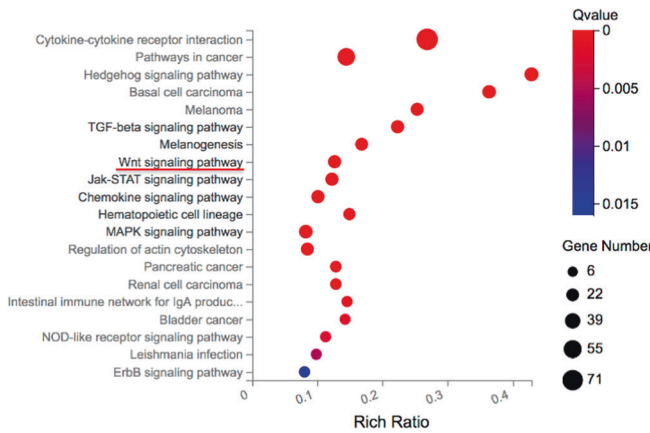
A. Differential gene expression



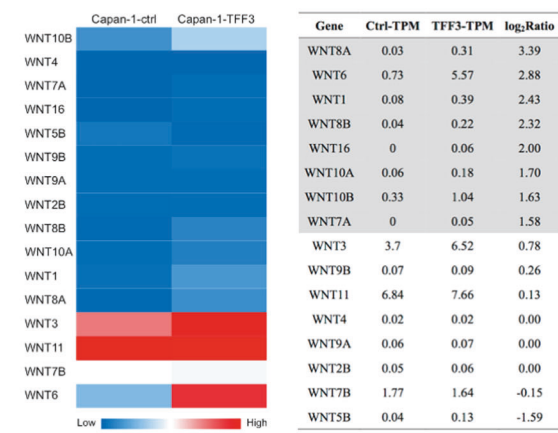
B. Gene set enrichment



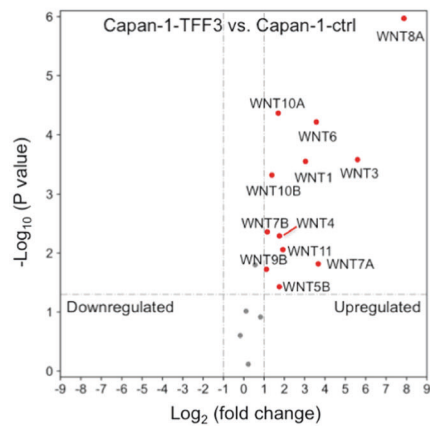
C. KEGG-pathway



D. Differential gene expression



E. QPCR



F. Western blot

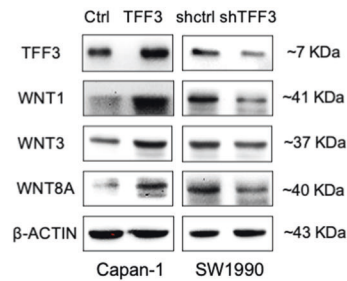


Fig. 5 TFF3 induced WNT ligand expression in PDAC. **A** Volcano plot shows the differentially up- or downregulated genes between Capan-1-TFF3 and the control cells. Genes deemed statistically significant are highlighted in red. **B** Relevant gene set enrichment plots from gene set enrichment analysis of secreted factors (NES, normalized enrichment score). **C** KEGG-pathway analysis was performed to identify the molecular pathways with highly altered activities. **D** Heatmap for differential expression of WNT ligand genes between Capan-1-TFF3 and the control cells. **E** Volcano plot of the gene expression profile of WNT ligands in Capan-1-TFF3 and the control cells based on qPCR. Mean expression relative to β -actin was plotted according to the \log_2 fold change (X axis) and \log_{10} P value (Y axis). **F** Western blot analysis was performed to determine the protein expression level of WNT ligands in Capan-1-TFF3, SW1990-shTFF3, and the respective control cells. β -actin was used as input control.

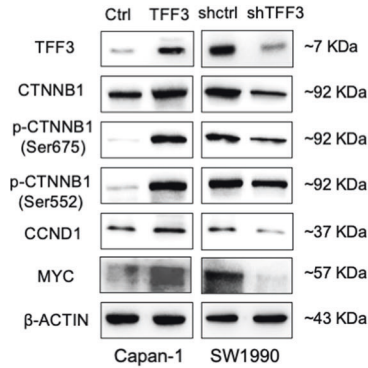
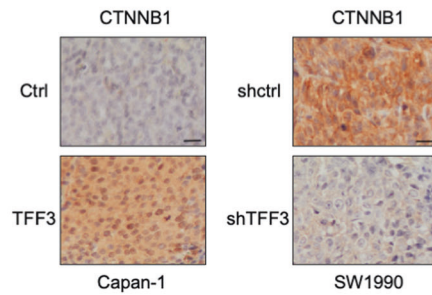
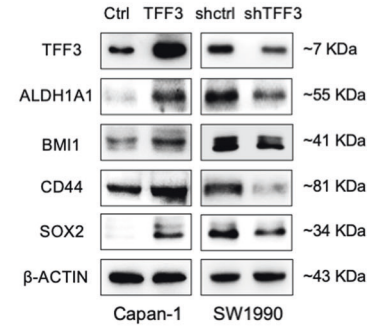
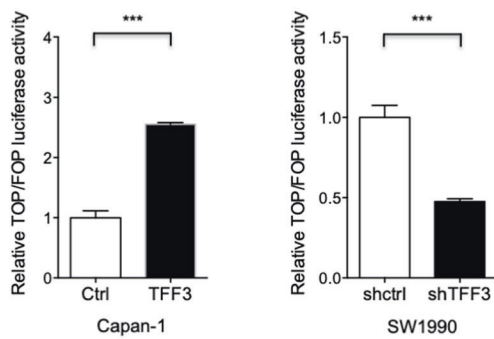
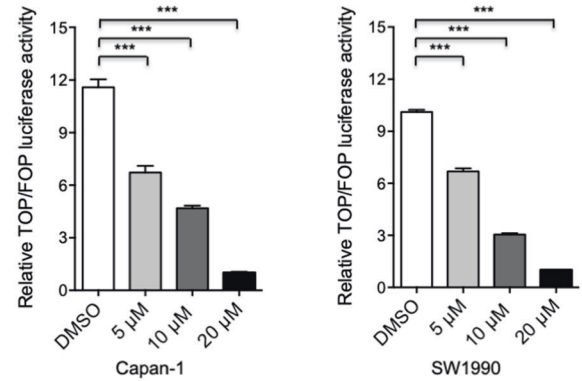
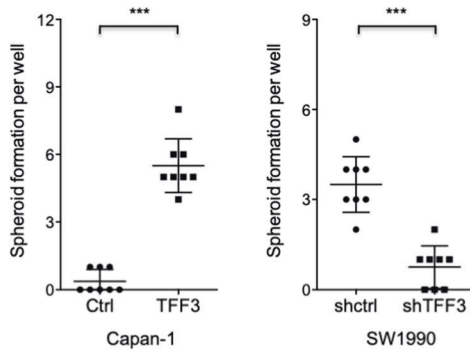
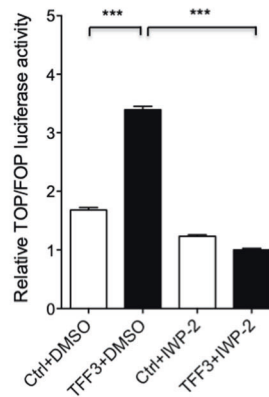
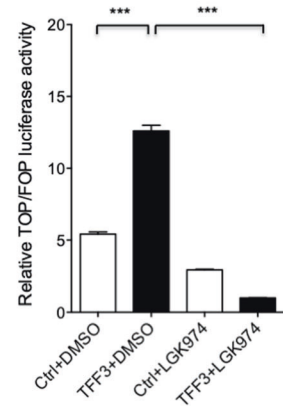
A. Western blot**B. Immunohistochemistry****E. Western blot****C. TOP/FOP-Flash activity****D. TOP/FOP-Flash activity****F. Spheroid formation****G. TOP/FOP-Flash activity****H. TOP/FOP-Flash activity**

Fig. 6 TFF3 activated WNT signaling by inducing WNT ligand expression in PDAC. **A** Western blot analysis was performed to determine the expression of WNT-related proteins in Capan-1-TFF3, SW1990-shTFF3, and the corresponding control cells. β -actin was used as input control. **B** Representative micrographs of IHC staining for CTNNB1 in the indicated xenografts. Scale bar, 20 μ m. **C** Relative TOP/FOP luciferase activity analysis was performed to determine the change of CTNNB1/TCF transcription activity in Capan-1-TFF3, SW1990-shTFF3, and the respective control cells. **D** Relative TOP/FOP luciferase activity analysis was performed to determine the change of CTNNB1/TCF transcription activity in Capan-1 and SW1990 cells after AMPC treatment. **E** Western blot analysis was performed to determine the protein expression of stemness-associated genes in Capan-1-TFF3, SW1990-shTFF3, and the corresponding control cells. β -actin was used as input control. **F** Spheroid formation assay for Capan-1-TFF3, SW1990-shTFF3, and the respective control cells. **G, H** TOP/FOP luciferase activity analysis was performed to determine the change of CTNNB1/TCF transcription activity in Capan-1-TFF3 and the control cells after the suppression of WNT ligand secretion with 10 μ M IWP-2 (**G**) or LGK-974 (**H**) treatment for 48 hours.

proteins (as exemplars), whereas depletion of *TFF3* in SW1990 cells reduced their protein expression (Fig. 5F and S03). These results were consistent with that observed in RNA-seq, verifying that *TFF3* promotes WNT ligand expression.

TFF3 activates WNT signaling by inducing WNT ligand expression in PDAC

It was further investigated whether *TFF3* activates WNT signaling in PDAC. As shown in Fig. 6A, S5A, and S04, it was observed that

forced expression of *TFF3* in Capan-1 cells increased the protein expression of CTNNB1 (β -CATENIN), a key component of the canonical WNT pathway, while depletion of *TFF3* in SW1990 cells reduced its expression. This finding was further supported by IHC staining of CTNNB1 protein in xenografts generated in the xenograft models described above (Fig. 6B). A positive correlation between the protein expression levels of *TFF3* and CTNNB1 in PDAC cell lines (Fig. S5B and S05) was also observed. In addition, forced expression of *TFF3* in Capan-1 cells also increased the levels of phosphorylated forms of CTNNB1 (Ser675 and Ser552) presumed to be the active forms of CTNNB1 (Fig. 6A). Consistent results were obtained in SW1990 cells after depletion of *TFF3* or after AMPC treatment (Figs. 6A, S5C, and S06). As shown by luciferase reporter activity (TOP/FOP Flash) assays, forced expression of *TFF3* in Capan-1 cells also activated CTNNB1/TCF transcriptional activity, while depletion of *TFF3* in SW1990 cells suppressed this transcriptional activity (Fig. 6C). This was corroborated by the decreased CTNNB1/TCF transcriptional activity observed in Capan-1 and SW1990 cells after AMPC treatment (Fig. 6D). As shown in Fig. 6A, forced expression of *TFF3* significantly increased the protein expression of WNT target genes *CCND1* and *MYC*, whereas depletion of *TFF3* reduced their expression. Consistent results were obtained in SW1990 cells after AMPC treatment (Fig. S5C and S06). Hence, *TFF3* activates the WNT pathway signaling in PDAC cells.

It has been reported that the WNT pathway promotes cancer stem cell (CSC)-like behavior in multiple cancers [40–42], and hence it was next determined whether *TFF3* regulates CSC-like behavior in PDAC. As shown in Supplementary Fig. S5D, forced expression of *TFF3* in Capan-1 cells significantly increased the mRNA expression of several common stemness-associated genes, such as *BMI1*, *CD9*, *CD44*, and *SOX2* [43, 44]. Conversely, depletion of *TFF3* in SW1990 cells attenuated the expression of these genes at the mRNA level (Fig. S5D). The expression changes of stemness-associated genes were further confirmed at the protein level (Fig. 6E and S07). In addition, forced expression of *TFF3* significantly promoted the spheroid formation and the tumor-initiating capacity of Capan-1 cells, whereas depletion of *TFF3* in SW1990 cells significantly impaired these properties (Figs. 6F and S5E). Hence, *TFF3* promotes CSC-like behavior in PDAC cells.

It was further determined whether *TFF3* activates WNT signaling by inducing WNT ligand expression in PDAC. IWP-2 and LGK-974 are two small-molecule inhibitors, both of which block WNT ligand secretion by inhibiting PORCN enzymatic activity [45]. As shown in Fig. 6G, IWP-2 treatment attenuated the increased CTNNB1/TCF transcriptional activity of Capan-1 cells observed with forced expression of *TFF3*. Similar results were observed after LGK-974 treatment (Fig. 6H). Hence, *TFF3* activates the WNT signaling pathway by inducing WNT ligand expression.

TFF3 promotes oncogenic functions of PDAC cells in a WNT-dependent manner

Previous studies have reported that WNT signaling promotes PDAC progression [40, 46]. Consistently, depletion of CTNNB1 via RNA interference resulted in significantly decreased proliferation of SW1990 cells (Fig. S6A, B, C, and S08). Similar effects were also observed in SW1990 cells treated with ICG-001 (Fig. 7A), a common small-molecule inhibitor of WNT pathway that functions by specifically inhibiting CTNNB1/TCF transcriptional activity. As observed in Fig. 7B, treatment with ICG-001 abrogated the increased proliferation of Capan-1 cells with forced expression of *TFF3*. Consistently, ICG-001 treatment also decreased the enhanced 3D growth of Capan-1-*TFF3* cells compared with that in the control cells (Fig. 7C). In addition, it was observed that ICG-001 treatment abrogated the enhanced spheroid formation and tumor-initiating capacities of Capan-1 cells with forced expression of *TFF3* (Fig. 7D, E). Western blot analysis further indicated that

depletion of CTNNB1 prevented the increased WNT-associated gene expression produced by forced expression of *TFF3* in Capan-1 cells (Fig. 7F and S09). Hence, *TFF3* promotes the oncogenic function of PDAC cells in a WNT-dependent manner.

Combination treatment of AMPC and WNT inhibitor suppresses xenograft growth and potentiates the efficacy of gemcitabine

Combination therapy improves therapeutic efficacy compared with single-drug treatment by enhancing cytotoxicity and reducing the development of drug resistance in cancer cells [47, 48]. The therapeutic efficacy of AMPC in combination with ICG-001 was, therefore, first determined in a 3D-Matrigel growth model. The established colonies were treated with AMPC, ICG-001, or a combination of AMPC and ICG-001. On the 9th day, a significant difference in the colony volume was observed in the AMPC-treated group compared with the vehicle group (Fig. 8A). Moreover, combination treatment of AMPC and ICG-001 led to smaller colony volumes compared with colonies treated with only AMPC or ICG-001 alone (Fig. 8A).

Gemcitabine is a current standard of therapy for PDAC. However, drug resistance and side effects have seriously limited its therapeutic efficacy [49, 50]. Therefore, it was investigated whether a combination treatment of AMPC and ICG-001 would enhance the inhibitory effect of gemcitabine. It was observed that the triple combination of AMPC, ICG-001, and gemcitabine significantly reduced the colony volume compared with colonies co-treated with AMPC and ICG-001 or treated with a single drug (Fig. 8A), indicating that combination treatment of AMPC and ICG-001 enhanced the efficacy of gemcitabine in PDAC.

It was next determined whether the enhanced efficacy of combination treatment with AMPC and ICG-001 would also be observed in the SW1990 xenograft model. Xenograft-bearing mice were randomized into the vehicle, single-drug, double-drug, or triple-drug groups, and were treated with intraperitoneal injections of vehicle, AMPC, ICG-001, gemcitabine, or combination treatment. After 2 weeks of treatment, AMPC treatment significantly inhibited xenograft growth compared with the vehicle group (Fig. 8B and Supplementary Fig. 7A), similar to that previously observed after depletion of *TFF3* (Fig. 3F, G). Furthermore, combination treatment with AMPC and ICG-001 exhibited significantly stronger effects on xenograft growth inhibition than the vehicle or single-drug group (Fig. 8B). The triple combination of AMPC, ICG-001, and gemcitabine resulted in the highest inhibition of xenograft growth compared with any other group (Fig. 8B). These results were also confirmed by the measurement of xenograft weight at the termination of the experiments (Fig. 8C). The drug treatments were well tolerated, as observed by lack of significant change of body weight and the weights of representative major organs, including liver, kidney, and lung (Fig. 8D and Supplementary Fig. 7A).

AMPC treatment reduces cellular and secreted *TFF3* levels [18, 24]. To determine the efficacy of AMPC, the serum levels of human *TFF3* derived from xenograft animals were therefore measured. As shown in Fig. 8E, all groups treated with AMPC exhibited lower levels of *TFF3* compared with groups without AMPC treatment, including the single ICG-001 or gemcitabine group with reduced xenograft volume. Similar results were obtained by IHC analysis for *TFF3* in xenograft tissue samples (Fig. 8F). AMPC treatment also significantly reduced CTNNB1 expression in xenograft tissues compared with non-treated controls (Fig. 8F). Combination treatment with AMPC and ICG-001 resulted in significantly reduced xenograft cell proliferation and increased apoptosis compared with the vehicle and single-drug groups (Figs. 8G, H). The triple combination of AMPC, ICG-001, and gemcitabine led to the lowest percentage of Ki67-positive cells and the highest percentage of TUNEL-positivity

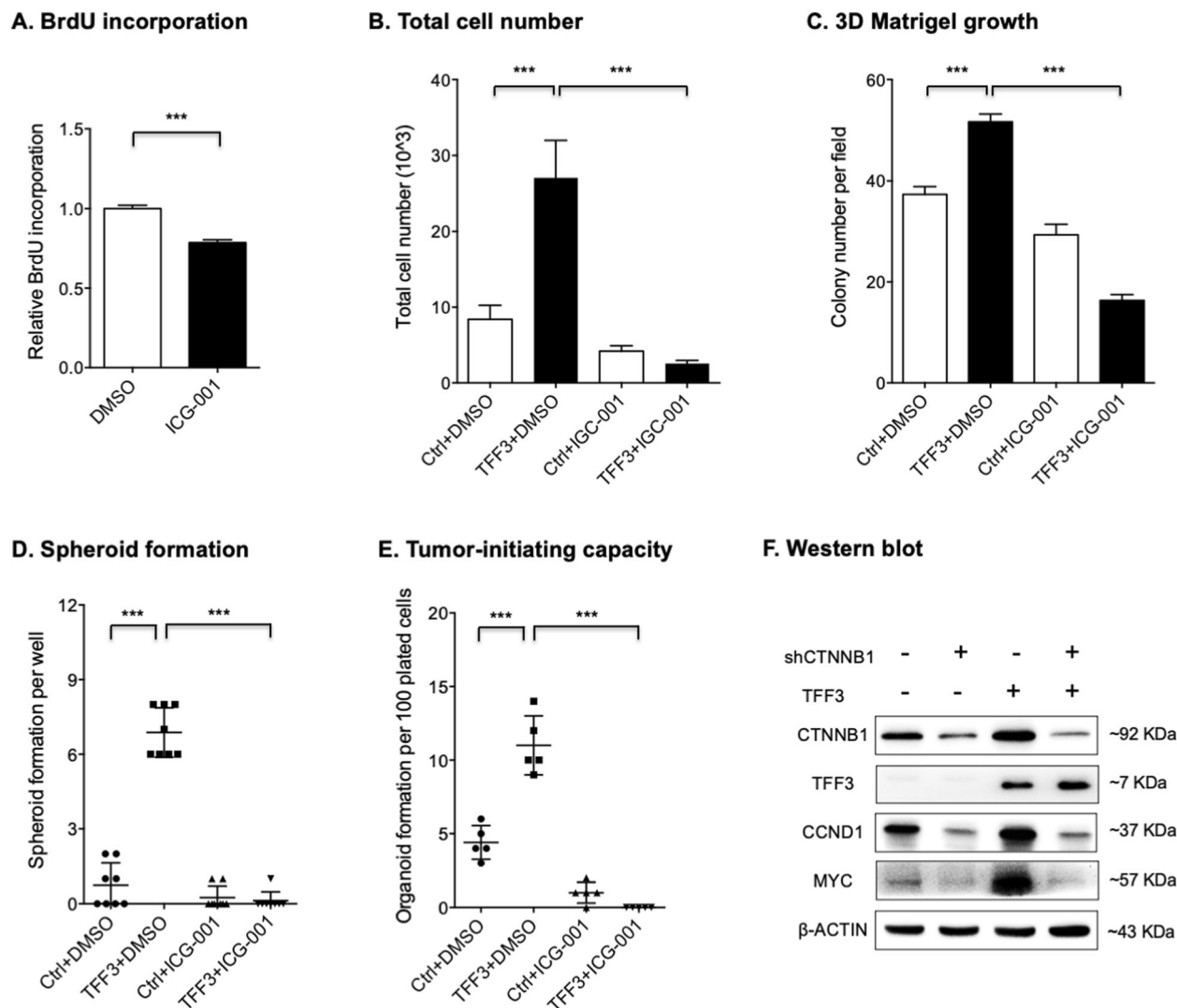


Fig. 7 TFF3 promoted oncogenic functions of PDAC cells in a WNT-dependent manner. **A** BrdU analysis for SW1990 cells treated with 2 μ M ICG-001 for 48 hours. **B, C** Total cell number counting (**B**) and 3D-Matrigel (**C**) analysis showed that forced expression of TFF3 in Capan-1 cells significantly promoted cell proliferation and 3D growth, respectively, and 2 μ M ICG-001 treatment for 48 hours abrogated these processes. **D, E** Spheroid (**D**) and organoid (**E**) formation assay showed that forced expression of TFF3 in Capan-1 cells significantly promoted colony formation and tumor-initiating capabilities respectively, and 2 μ M ICG-001 treatment for 48 hours reversed these processes. **F** Western blot analysis showed that depletion of CTNNB1 prevented the upregulation of WNT-associated gene expression produced by forced expression of TFF3 in Capan-1 cells. β -actin was used as input control.

compared with other groups (Fig. 8G, H). Hence, combination treatment of AMPC and ICG-001 suppresses xenograft growth and potentiates the therapeutic efficacy of gemcitabine in vivo.

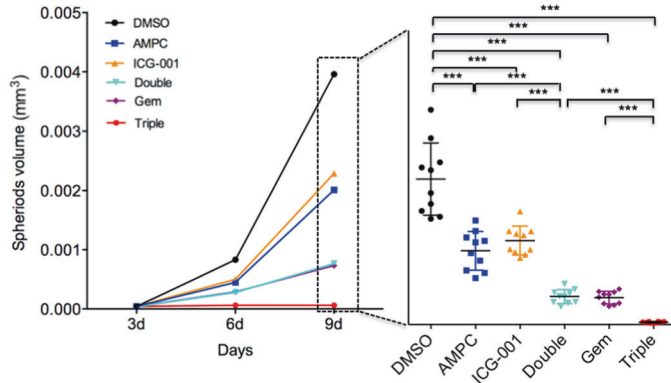
DISCUSSION

There are still no FDA-approved drugs that effectively target the most commonly mutated genes (*KRAS*, *CDKN2A*, *TP53*, and *SMAD4*) in PDAC, although Sotorasib (a *KRAS*-G12C inhibitor) was recently approved for advanced non-small cell lung cancer [1, 51]. Hence, characterization of novel potent and non-mutated oncogenic drivers that contribute to PDAC progression is necessary to potentially improve targeted therapeutic outcomes. Consistent with recent studies [31, 32], TFF3 exhibited an elevated expression in PDAC compared with that in normal tissues. The data herein further revealed that TFF3 expression in PDAC, regardless of underlying genetic mutations, was positively correlated with worse overall survival, implying that TFF3 may function as an independent prognostic indicator for PDAC.

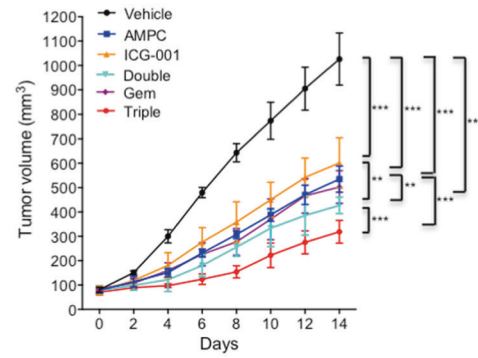
AMPC was used herein to determine the potential efficacy of pharmacological targeting TFF3 in PDAC. It was observed that AMPC significantly impaired PDAC cell number increases in vitro and in vivo, consistent with previous observations [10, 18, 24]. Hence, precision targeting of TFF3 may be a potential therapeutic strategy for PDAC. It should be noted that compared with ER⁺ mammary carcinoma cells, AMPC appeared less efficacious in the PDAC cell lines used herein. However, considering the limited options that are available for PDAC treatment, this study may expand therapeutic opportunities for PDAC.

Recently, several studies reported that TFF3 promoted CSC-like properties in the colorectal, hepatocellular, lung, and mammary carcinoma [16, 18, 20]. However, the mechanism by which TFF3 promotes CSC-like properties remained to be elucidated. It was observed herein that TFF3 activated the WNT signaling pathway by enhancing WNT ligand expression. Hence, at least in PDAC, TFF3 might promote CSC-like behavior by activating the WNT pathway. There are still no FDA-approved drugs that target the WNT pathway for cancer

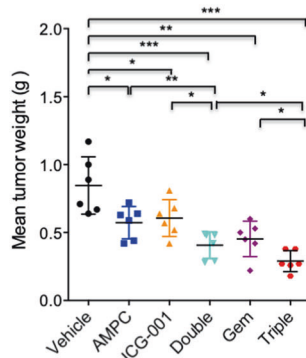
A. 3D Matrigel



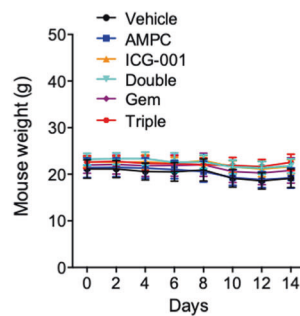
B. Tumor growth curve



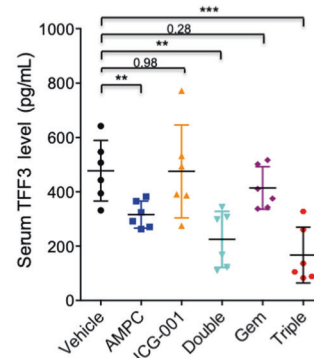
C. Tumor weight



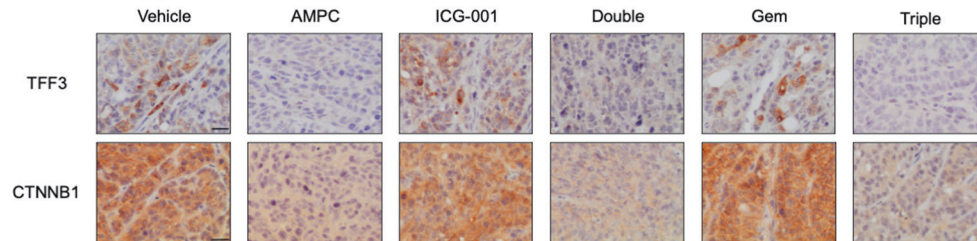
D. Mouse weight



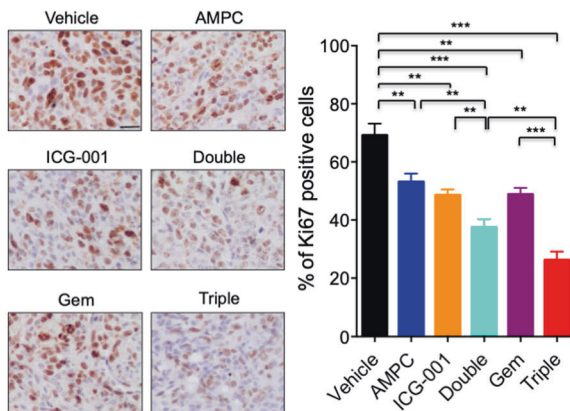
E. ELISA



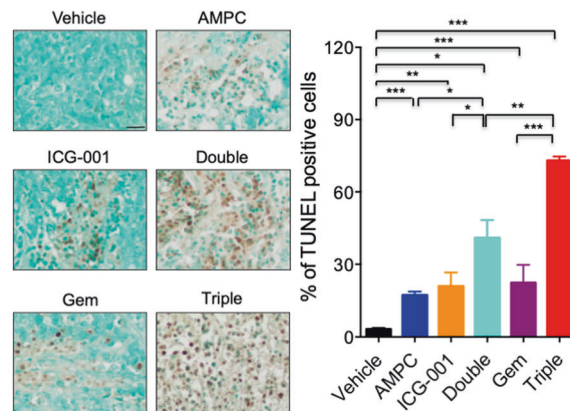
F. Immunohistochemistry



G. Ki67



H. TUNEL



therapy. Inhibition of the WNT pathway produces considerable side effects as the WNT pathway is critical for the maintenance of normal stem cells [52]. Hence, combination therapy with a low-dose WNT inhibitor and other therapeutic agents may prove to be more clinically useful [53]. In the present study, combination treatment with AMPC and WNT inhibitor

exhibited significantly stronger effects on xenograft growth inhibition than the vehicle or single-drug groups. In addition, it was observed that the combination treatments were well tolerated.

In conclusion, the oncogenic function of TFF3 in PDAC progression has been systematically elucidated herein.

Fig. 8 Combination treatment of AMPC and WNT inhibitor suppressed xenograft growth and potentiated the efficacy of gemcitabine. **A** 3D-Matrigel growth analysis for SW1990 cells after AMPC, ICG-001, AMPC + ICG-001 (Double), gemcitabine (Gem) or AMPC + ICG-001 + Gem (Triple) treatment. The graph shows the spheroid volume in each group. Data represent means \pm SD from at least three independent experiments. * $P < 0.05$, ** $P < 0.01$, and *** $P < 0.001$. **B** Growth curve of SW1990-derived xenografts after treatment with vehicle, AMPC, ICG-001, Double, Gem, or Triple. $n = 6$ mice per group. Data are represented as means \pm SEM. * $P < 0.05$, ** $P < 0.01$, and *** $P < 0.001$. **C** Weights of the isolated SW1990-derived xenografts at the termination of the experiments. **D** Body weights of the mice during the treatment period. $n = 6$ mice per group. Data are represented as mean \pm SD. * $P < 0.05$, ** $P < 0.01$, and *** $P < 0.001$. **E** ELISA analysis for serum levels of human TFF3 derived from xenografts. **F** Representative micrographs of IHC staining for TFF3 and CTNNB1 in the indicated xenografts. Scale bar, 20 μ m. **G** Representative micrographs and quantitative assay of IHC staining results for Ki67 in the indicated xenografts. Scale bar, 20 μ m. Data are represented as means \pm SD. * $P < 0.05$, ** $P < 0.01$, and *** $P < 0.001$. **H** Representative micrographs and quantitative assay of TUNEL staining results in the indicated xenografts. Scale bar, 20 μ m. Data are represented as means \pm SD. * $P < 0.05$, ** $P < 0.01$, and *** $P < 0.001$.

Considering the paucity of knowledge of the specific determinants promoting PDAC development/progression, this study provides novel insights on TFF3 regulation of PDAC cell function and provides a rationale for considering the use of TFF3 inhibitors in the therapy of PDAC.

DATA AND MATERIALS AVAILABILITY

The data sets used in this study are available from the corresponding author on reasonable request. Requests for materials should be addressed to Vijay Pandey or Peter E. Lobie.

REFERENCES

- Siegel RL, Miller KD, Jemal A. Cancer statistics, 2018. *CA Cancer J Clin*. 2018;68:7–30.
- Kleeff J, Korc M, Apte M, La Vecchia C, Johnson CD, Biankin AV, et al. Pancreatic cancer. *Nat Rev Dis Prim*. 2016;2:16022.
- Witkiewicz AK, McMillan EA, Balaji U, Baek G, Lin WC, Mansour J, et al. Whole-exome sequencing of pancreatic cancer defines genetic diversity and therapeutic targets. *Nat Commun*. 2015;6:6744.
- Pandey V, Zhang M, You M, Zhang W, Chen R, Zhang W, et al. Expression of two non-mutated genetic elements is sufficient to stimulate oncogenic transformation of human mammary epithelial cells. *Cell Death Dis*. 2018;9:1147.
- Perry JK, Kannan N, Grandison PM, Mitchell MD, Lobie PE. Are trefoil factors oncogenic? *Trends Endocrinol Metab*. 2008;19:74–81.
- Dieckow J, Brandt W, Hattermann K, Schob S, Schulze U, Mentlein R, et al. CXCR4 and CXCR7 mediate TFF3-induced cell migration independently from the ERK1/2 signaling pathway. *Invest Ophthalmol Vis Sci*. 2016;57:56–65.
- Belle NM, Ji Y, Herbine K, Wei Y, Park J, Zullo K, et al. TFF3 interacts with LINGO2 to regulate EGFR activation for protection against colitis and gastrointestinal helminths. *Nat Commun*. 2019;10:4408.
- Cui HY, Wang SJ, Song F, Cheng X, Nan G, Zhao Y, et al. CD147 receptor is essential for TFF3-mediated signaling regulating colorectal cancer progression. *Signal Transduct Target Ther*. 2021;6:268.
- Perera O, Evans A, Pertziger M, MacDonald C, Chen H, Liu DX, et al. Trefoil factor 3 (TFF3) enhances the oncogenic characteristics of prostate carcinoma cells and reduces sensitivity to ionising radiation. *Cancer Lett*. 2015;361:104–11.
- Chen RM, Chiou YS, Chong QY, Poh HM, Tan TZ, Zhang MY, et al. Pharmacological inhibition of TFF3 enhances sensitivity of CMS4 colorectal carcinoma to 5-fluorouracil through inhibition of p44/42 MAPK. *Int J Mol Sci*. 2019;20:6215.
- Yusufu A, Shayimu P, Tuerdi R, Fang C, Wang F, Wang H. TFF3 and TFF1 expression levels are elevated in colorectal cancer and promote the malignant behavior of colon cancer by activating the EMT process. *Int J Oncol*. 2019;55:789–804.
- Yusup A, Huji B, Fang C, Wang F, Dadihan T, Wang HJ, et al. Expression of trefoil factors and TWIST1 in colorectal cancer and their correlation with metastatic potential and prognosis. *World J Gastroenterol*. 2017;23:110–20.
- Pandey V, Zhang M, Chong QY, You M, Raquib AR, Pandey AK, et al. Hypomethylation associated enhanced transcription of trefoil factor-3 mediates tamoxifen-stimulated oncogenicity of ER⁺ endometrial carcinoma cells. *Oncotarget* 2017;8:77268–91.
- Taniguchi Y, Kurokawa Y, Takahashi T, Mikami J, Miyazaki Y, Tanaka K, et al. Prognostic value of Trefoil factor 3 expression in patients with gastric cancer. *World J Surg*. 2018;42:3997–4004.
- Kirikoshi H, Katoh M. Expression of TFF1, TFF2 and TFF3 in gastric cancer. *Int J Oncol*. 2002;21:655–9.
- You ML, Chen YJ, Chong QY, Wu MM, Pandey V, Chen RM, et al. Trefoil factor 3 mediates of oncogenicity and chemoresistance in hepatocellular carcinoma is AKT-BCL-2 dependent. *Oncotarget* 2017;8:39323–44.
- Okada H, Kimura MT, Tan D, Fujiwara K, Igarashi J, Makuuchi M, et al. Frequent trefoil factor 3 (TFF3) overexpression and promoter hypomethylation in mouse and human hepatocellular carcinomas. *Int J Oncol*. 2005;26:369–77.
- Zhang M, Wang B, Chong QY, Pandey V, Guo Z, Chen RM, et al. A novel small-molecule inhibitor of trefoil factor 3 (TFF3) potentiates MEK1/2 inhibition in lung adenocarcinoma. *Oncogenesis* 2019;8:65.
- Wang XN, Wang SJ, Pandey V, Chen P, Li Q, Wu ZS, et al. Trefoil factor 3 as a novel biomarker to distinguish between adenocarcinoma and squamous cell carcinoma. *Medicine*. 2015;94:e860.
- Kannan N, Kang J, Kong X, Tang J, Perry JK, Mohankumar KM, et al. Trefoil factor 3 is oncogenic and mediates anti-estrogen resistance in human mammary carcinoma. *Neoplasia* 2010;12:1041–53.
- May FE, Westley BR. TFF3 is a valuable predictive biomarker of endocrine response in metastatic breast cancer. *Endocr Relat Cancer*. 2015;22:465–79.
- Thomsen KG, Lyng MB, Elias D, Vever H, Knoop AS, Lykkesfeldt AE, et al. Gene expression alterations associated with outcome in aromatase inhibitor-treated ER⁺ early-stage breast cancer patients. *Breast Cancer Res Treat*. 2015;154:483–94.
- Garraway IP, Seligson D, Said J, Horvath S, Reiter RE. Trefoil factor 3 is overexpressed in human prostate cancer. *Prostate* 2004;61:209–14.
- Chong QY, You ML, Pandey V, Banerjee A, Chen YJ, Poh HM, et al. Release of HER2 repression of trefoil factor 3 (TFF3) expression mediates trastuzumab resistance in HER2⁺/ER⁺ mammary carcinoma. *Oncotarget* 2017;8:74188–208.
- Poh HM, Chiou YS, Chong QY, Chen RM, Rangappa KS, Ma L, et al. Inhibition of TFF3 enhances sensitivity-and overcomes acquired resistance-to doxorubicin in estrogen receptor-positive mammary carcinoma. *Cancers (Basel)*. 2019;11:1528.
- Lau WH, Pandey V, Kong X, Wang XN, Wu Z, Zhu T, et al. Trefoil factor-3 (TFF3) stimulates de novo angiogenesis in mammary carcinoma both directly and indirectly via IL-8/CXCR2. *PLoS One*. 2015;10:e0141947.
- Morito K, Nakamura J, Kitajima Y, Kai K, Tanaka T, Kubo H, et al. The value of trefoil factor 3 expression in predicting the long-term outcome and early recurrence of colorectal cancer. *Int J Oncol*. 2015;46:563–8.
- Meng JR, Tang HZ, Zhou KZ, Shen WH, Guo HY. TFF3 and survivin expressions associate with a lower survival rate in gastric cancer. *Clin Exp Med*. 2013;13:297–303.
- Ding A, Zhao W, Shi X, Yao R, Zhou F, Yue L, et al. Impact of NPM, TFF3 and TACC1 on the prognosis of patients with primary gastric cancer. *PLoS One*. 2013;8:e82136.
- Pandey V, Wu ZS, Zhang M, Li R, Zhang J, Zhu T, et al. Trefoil factor 3 promotes metastatic seeding and predicts poor survival outcome of patients with mammary carcinoma. *Breast Cancer Res*. 2014;16:429.
- Terris B, Blaveri E, Crnogorac-Jurcevic T, Jones M, Missiaglia E, Ruzsniowski P, et al. Characterization of gene expression profiles in intraductal papillary-mucinous tumors of the pancreas. *Am J Pathol*. 2002;160:1745–54.
- Jahan R, Ganguly K, Smith LM, Atri P, Carmichael J, Sheinin Y, et al. Trefoil factor(s) and CA19.9: a promising panel for early detection of pancreatic cancer. *EBioMedicine* 2019;42:375–85.
- Cheng F, Su L, Yao C, Liu L, Shen J, Liu C, et al. SIRT1 promotes epithelial-mesenchymal transition and metastasis in colorectal cancer by regulating Fra-1 expression. *Cancer Lett*. 2016;375:274–83.
- Tang JZ, Zuo ZH, Kong XJ, Steiner M, Yin Z, Perry JK, et al. Signal transducer and activator of transcription (STAT)-5A and STAT5B differentially regulate human mammary carcinoma cell behavior. *Endocrinology* 2010;151:43–55.
- Kilkenny C, Browne W, Cuthill IC, Emerson M, Altman DG, National Centre for the Replacement, Refinement and Reduction of Animals in Research. Animal research: reporting in vivo experiments-the ARRIVE guidelines. *J Cereb Blood Flow Metab*. 2011;31:991–3.
- Pandey V, Wang B, Mohan CD, Raquib AR, Rangappa S, Srinivasa V, et al. Discovery of a small-molecule inhibitor of specific serine residue BAD phosphorylation. *Proc Natl Acad Sci USA*. 2018;115:E10505–E10514.

37. Jackerott M, Lee YC, Møllgård K, Kofod H, Jensen J, Rohleder S, et al. Trefoil factors are expressed in human and rat endocrine pancreas: differential regulation by growth hormone. *Endocrinology* 2006;147:5752–9.
38. Fueger PT, Schisler JC, Lu D, Babu DA, Mirmira RG, Newgard CB, et al. Trefoil factor 3 stimulates human and rodent pancreatic islet beta-cell replication with retention of function. *Mol Endocrinol.* 2008;22:1251–9.
39. Muskett FW, May FE, Westley BR, Feeney J. Solution structure of the disulfide-linked dimer of human intestinal trefoil factor (TFF3): the intermolecular orientation and interactions are markedly different from those of other dimeric trefoil proteins. *Biochemistry* 2003;42:15139–47.
40. Hou P, Ma X, Zhang Q, Wu CJ, Liao W, Li J, et al. USP21 deubiquitinase promotes pancreas cancer cell stemness via Wnt pathway activation. *Genes Dev.* 2019;33:1361–6.
41. Zhan T, Ambrosi G, Wandmacher AM, Rauscher B, Betge J, Rindtorff N, et al. MEK inhibitors activate Wnt signalling and induce stem cell plasticity in colorectal cancer. *Nat Commun.* 2019;10:2197.
42. Murillo-Garzón V, Kypka R. WNT signalling in prostate cancer. *Nat Rev Urol.* 2017;14:683–96.
43. Wang VM, Ferreira RMM, Almagro J, Evan T, Legrave N, Zaw Thin M, et al. CD9 identifies pancreatic cancer stem cells and modulates glutamine metabolism to fuel tumour growth. *Nat Cell Biol.* 2019;21:1425–35.
44. Zhang Z, Han H, Rong Y, Zhu K, Zhu Z, Tang Z, et al. Hypoxia potentiates gemcitabine-induced stemness in pancreatic cancer cells through AKT/Notch1 signaling. *J Exp Clin Cancer Res.* 2018;37:291.
45. Leung EY, Askarian-Amiri ME, Sarkar D, Ferraro-Peyret C, Joseph WR, Finlay GJ, et al. Endocrine therapy of estrogen receptor-positive breast cancer cells: early differential effects on stem cell markers. *Front Oncol.* 2017;7:184.
46. Tang B, Yang Y, Kang M, Wang Y, Wang Y, Bi Y, et al. m6A demethylase ALKBH5 inhibits pancreatic cancer tumorigenesis by decreasing WIF-1 RNA methylation and mediating Wnt signaling. *Mol Cancer.* 2020;19:3.
47. Sun C, Fang Y, Yin J, Chen J, Ju Z, Zhang D, et al. Rational combination therapy with PARP and MEK inhibitors capitalizes on therapeutic liabilities in RAS mutant cancers. *Sci Transl Med.* 2017;9:eaal5148.
48. Kuninty PR, Bansal R, De Geus SWL, Mardhian DF, Schnitter J, van Baarlen J, et al. ITGA5 inhibition in pancreatic stellate cells attenuates desmoplasia and potentiates efficacy of chemotherapy in pancreatic cancer. *Sci Adv.* 2019;5:eaax2770.
49. Liu W, Mao Y, Zhang X, Wang Y, Wu J, Zhao S, et al. RGDV-modified gemcitabine: a nano-medicine capable of prolonging half-life, overcoming resistance and eliminating bone marrow toxicity of gemcitabine. *Int J Nanomed.* 2019;14:7263–79.
50. Ma T, Chen W, Zhi X, Liu H, Zhou Y, Chen BW, et al. USP9X inhibition improves gemcitabine sensitivity in pancreatic cancer by inhibiting autophagy. *Cancer Lett.* 2018;436:129–38.
51. Nakajima EC, Drezner N, Li X, Mishra-Kalyani PS, Liu Y, Zhao H, et al. FDA approval summary: sotorasib for KRAS G12C-mutated metastatic NSCLC. *Clin Cancer Res.* 2021; <https://doi.org/10.1158/1078-0432.CCR-21-3074>.
52. Krishnamurthy N, Kurzrock R. Targeting the Wnt/beta-catenin pathway in cancer: update on effectors and inhibitors. *Cancer Treat Rev.* 2018;62:50–60.
53. Dotan E, Cardin DB, Lenz HJ, Messersmith W, O'Neil B, Cohen SJ, et al. Phase Ib study of Wnt inhibitor ipafricept with gemcitabine and nab-paclitaxel in patients with previously untreated stage IV pancreatic cancer. *Clin Cancer Res.* 2020;26:5348–57.

AUTHOR CONTRIBUTIONS

P.E.L., V.P., and F.C. designed the study; Basappa synthesized AMPC. F.C., X.W., Y.-S.C., C.H., and H.G. performed the experiments; F.C., X.W., Y.-S.C., C.H., Y.Q.T., T.Z., and P.E.L. analyzed the data; F.C. wrote the draft; P.E.L., V.P., X.W., and Y.Q.T. revised the paper. All authors read and approved the final manuscript.

FUNDING

This work was supported by the Shenzhen Key Laboratory of Innovative Oncotherapeutics (ZDSYS20200820165400003) (Shenzhen Science and Technology

Innovation Commission), China; Shenzhen Development and Reform Commission Subject Construction Project ([2017]1434), China; Guangdong Basic and Applied Basic Research Foundation (2020A1515111064), China; Overseas Research Cooperation Project (HW2020008) (Tsinghua Shenzhen International Graduate School), China; TBSI Faculty Start-up Funds, China and The Shenzhen Bay Laboratory, China.

COMPETING INTERESTS

Peter E. Lobie and Tao Zhu have previously consulted for Perseis Therapeutics Ltd. Peter E. Lobie are named on PCT application numbers WO 2006/69253 and WO 2008/042435 and US provisional application number 61/059558 and derivatives thereof. Vijay Pandey, Basappa, and Peter E. Lobie are named as inventors on PCT application WO/2018/226155 (PCT/SG2018/050277), Compounds, As Inhibitors of TFF3 Dimerization, Methods and Applications Thereof (and derivatives thereof including US Patent 11,141,402). Peter E. Lobie is an equity holder in Sinotar Pharmaceuticals Ltd which currently holds PCT/SG2018/050277 and derivatives thereof including issued US Patent no. 11,141,402.

ETHICS APPROVAL AND CONSENT TO PARTICIPATE

Consent for the use of the tissue samples and clinical data was obtained by Outdo Bio-Tech Co., Ltd. (Shanghai, China). All animal experiments were approved by the Institutional Animal Care and Use Committee of the Laboratory Animal Centre of Peking University Shenzhen Graduate School (YW) and the Ethics Committee of Tsinghua Shenzhen International Graduate School (Ethical Development no. 37, year 2019).

CONSENT FOR PUBLICATION

All of the study participants have given consent to publish this paper.

ADDITIONAL INFORMATION

Supplementary information The online version contains supplementary material available at <https://doi.org/10.1038/s41419-022-04700-4>.

Correspondence and requests for materials should be addressed to Vijay Pandey or Peter E. Lobie.

Reprints and permission information is available at <http://www.nature.com/reprints>

Publisher's note Springer Nature remains neutral with regard to jurisdictional claims in published maps and institutional affiliations.



Open Access This article is licensed under a Creative Commons Attribution 4.0 International License, which permits use, sharing, adaptation, distribution and reproduction in any medium or format, as long as you give appropriate credit to the original author(s) and the source, provide a link to the Creative Commons license, and indicate if changes were made. The images or other third party material in this article are included in the article's Creative Commons license, unless indicated otherwise in a credit line to the material. If material is not included in the article's Creative Commons license and your intended use is not permitted by statutory regulation or exceeds the permitted use, you will need to obtain permission directly from the copyright holder. To view a copy of this license, visit <http://creativecommons.org/licenses/by/4.0/>.

© The Author(s) 2022